

Lattice dynamics of α -quartz*

M. E. Striefer and G. R. Barsch

Materials Research Laboratory and Department of Physics, The Pennsylvania State University, University Park, Pennsylvania 16802

(Received 17 March 1975)

The phonon dispersion curves, the temperature dependence of the Debye temperature, and the static elastic, dielectric, and piezoelectric constants of α -SiO₂ have been calculated from a modified rigid-ion model with an effective charge, with short-range central forces for the two Si-O interactions, for the four nearest-neighbor O-O interactions, for the four second-neighbor O-O interactions, and with three-body type angle-bending forces between nearest-neighbor O ions sharing a common Si-ion, and between Si-ions of adjacent tetrahedra and the linking O ion. The model involves 23 parameters which are reduced to 8 independent parameters by the six equilibrium conditions and by 15 constraints on the first and second derivatives of the interaction potential corresponding to the inner and outer O-O interactions. Using explicit expressions for the elastic constants and for the optical modes at zero wave vector, the eight free parameters were determined from a least-squares fit of the six elastic constants and of the 16 Raman and transverse ir frequencies. The effective charge of the Si ion is found to be 0.96 electronic charges, indicating a strong degree of covalency and/or screening. The model gives good over-all agreement for the elastic and optical data, rough agreement for the dielectric constants, and the correct sign and order of magnitude of the piezoelectric constants. The dispersion curves along [001] and the temperature dependence of the Debye temperature agree well with available experimental data, with moderate discrepancies occurring for the two acoustic branches and at low temperatures, respectively.

I. INTRODUCTION

The objective of this paper is to present the results of a consistent lattice-dynamical calculation of the optical frequencies, of the elastic, dielectric, and piezoelectric constants, of the phonon dispersion relations, and of the temperature dependence of the Debye temperature for α -quartz (SiO₂), which is based on a modified rigid-ion model and on the harmonic approximation. Although a considerable amount of theoretical work on the properties of α -quartz is available,^{1-17,21,22} in most cases only a few selected properties are considered and overly simplified models are used.

The majority of theoretical investigations deal with the explanation of the Raman and ir frequencies. Most of these¹⁻⁸ are force-constant models which include angle bending and stretching forces, but ignore long-range Coulomb forces which may be expected to be important in a partly ionic crystal such as quartz. This expectation is actually supported by more recent experimental Raman studies with laser excitation.^{9,10} In none of these investigations¹⁻⁸ are the elastic or piezoelectric constants treated.

Force-constant models have also been used for calculating the elastic^{11,12} and piezoelectric¹³⁻¹⁷ constants of α -quartz, but the consistency of these models with the optical frequencies has not been investigated. One of these models¹⁷ is a "rigid-stick-bar model" in which the nearest-neighbor distances (bond lengths) are assumed to be constant. In addition, the internal strain contribu-

tions to the elastic constants have been neglected in Ref. 11, although they may be quite large for other noncentrosymmetric crystal structures.¹⁸⁻²⁰

The most elaborate and consistent lattice-dynamical theory of α -quartz has been presented by Elcombe,^{21,22} who also measured the phonon dispersion relations for several low-lying branches along the threefold axis by means of inelastic neutron scattering. Elcombe calculated the optical-mode frequencies and the phonon dispersion curves on the basis of two models, a force-constant model and a rigid-ion model. Five of the six elastic constants were also determined from the long-wavelength slope of the dispersion curves. In the force-constant model only central forces between nearest Si-O and O-O neighbors are included and the difference between the various bond lengths of each type has been neglected. In the rigid-ion model the Coulomb forces are included and the ionic charge is scaled by means of an effective charge in order to account for deviations from complete ionic binding. The parameters of both models were determined from a least-squares fit of all 28 transverse and longitudinal optical-mode frequencies at the Brillouin-zone center. Both models gave fair to good fit to the optical frequencies, and fair agreement for the phonon dispersion relations. However, the calculated elastic constants are up to two times smaller than the experimental values for the force-constant model, and up to five times smaller for the rigid-ion model.²² These discrepancies may be expected to arise from the simplifying assumptions about the interatomic forces, especially

from the omission of angle-bending forces, and from the manner in which the parameters of the model were fitted to the experimental data. In addition, the equilibrium conditions for the structural parameters of quartz were not taken into account.²² Since the equilibrium conditions are intimately related to the rotational-invariance conditions for the coupling parameters, Elcombe's model refers to a crystal with nonvanishing internal stresses and does not satisfy the rotational-invariance conditions. The piezoelectric and dielectric constants were not calculated by Elcombe.²²

In the present paper we report on lattice-dynamical calculations on α -quartz which are based on an extended and refined version of Elcombe's modified rigid-ion model. The salient features of the new model are (i) a more differentiated model for the short-range forces which consist of central-force short-range interactions for the two Si-O distances, for the four second-neighbor O-O distances, and two kinds of three-body type angle-bending forces for the tetrahedral O-Si-O bond angle and for the Si-O-Si bond angle which describes the relative orientation of neighboring SiO_4 tetrahedra; (ii) including the rotational-invariance conditions for the coupling parameters and the equilibrium conditions for the internal strains, which made inclusion of the four second-neighbor O-O interactions necessary; (iii) explicit calculation of the elastic constants from the external and internal strain contributions; (iv) reduction of the 22 short-range parameters and of the effective charge to eight independent parameters by using the six equilibrium conditions (corresponding to the two lattice parameters and four structural parameters), and by using nine constraints on the first and second derivatives of the interaction potential for the first- and second-neighbor O-O interactions; (v) determination of the eight independent parameters from a simultaneous least-squares fit of the 16 Raman-active and transverse infrared-active frequencies (four Raman-active modes, four infrared-active modes and eight modes which are both Raman and infrared active), and of the six independent elastic constants to the 22 experimental data. On the basis of this model all (transverse and longitudinal) optical frequencies at zero wave vector, the elastic, dielectric, and piezoelectric constants, the phonon dispersion relations and frequency spectrum, and the temperature dependence of the Debye temperature were calculated. Other models were also tested, but models with fewer parameters (especially without angle-bending forces) did not give as good agreement as the eight-parameter model described, and models with more parameters did not result in a statistically significant improvement of the least-

squares fit. Inclusion of the angle-bending forces was found necessary for obtaining good agreement for the elastic constants and the deviations from the Cauchy relations. In addition, the fitting procedure used for determining the parameters of the model was examined. It was found that it is generally not difficult to account for one set of properties, but that it is much more difficult to develop a model which explains both optical and elastic properties well.

II. CRYSTAL SYMMETRY AND THEORETICAL MODEL

α -quartz occurs in two enantiomorphic crystal structures corresponding to the trigonal space groups²³ $D_3^4(P3_121)$ and $D_3^5(P3_221)$. There are three formula units (SiO_2) per unit cell. In Table I the coordinates of the atomic positions of a levorotatory crystal (space group D_3^4) as referred to a hexagonal unit cell with base vectors \vec{a}_1 , \vec{a}_2 , \vec{a}_3 are shown, where \vec{a}_1 and \vec{a}_2 form an angle of 120° , and \vec{a}_3 is perpendicular to \vec{a}_1 and \vec{a}_2 . The numerical values of the two lattice constants $a = |\vec{a}_1| = |\vec{a}_2|$ and $c = |\vec{a}_3|$, and of the four structural parameters u , x , y , z at 20°C are also included in Table I. The ions are labeled by the index $\kappa = 1, 2, \dots, 9$. The projection of the structure on the (001) plane in Fig. 1 shows the atomic positions and the arrangement of the SiO_4 tetrahedra in the unit cell.

In addition to the Coulomb interaction between the ions in the modified rigid-ion model considered here, central-force short-range interactions are

TABLE I. Equivalent positions, ion type, ion label κ , position coordinates (referred to the hexagonal axes of Fig. 1) and structural parameters for α -quartz ($u = 0.4698$,^a $x = 0.4145$,^a $y = 0.2662$,^a $z = 0.1189$,^a $a = 4.91304\text{\AA}$,^b $c = 5.40463\text{\AA}$ ^b).

Equivalent position	Ion type	κ	(x_1, x_2, x_3)
3a	Si	1	$(u, 0, 0)$
		2	$(0, u, \frac{2}{3})$
		3	$(\bar{u}, \bar{u}, \frac{1}{3})$
6c	O	4	(x, y, z)
		5	$(y, x, \frac{2}{3} - z)$
		6	$(\bar{y}, x - y, z + \frac{2}{3})$
		7	$(\bar{x}, y - x, \frac{1}{3} - z)$
		8	$(y - x, \bar{x}, z + \frac{1}{3})$
		9	$(x - y, \bar{y}, \bar{z})$

^a Reference 24.

^b Reference 23.

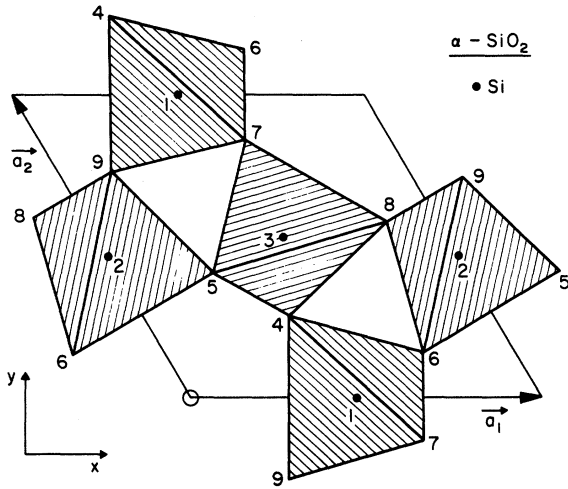


FIG. 1. Projection of structure of levorotatory α -quartz (D_3^h) on (001), showing the labeling of ions and the arrangement of the SiO_4 tetrahedra [after Landolt-Börnstein, in *Zahlenwerte und Funktionen*, edited by K. H. Hellwege (Springer-Verlag, Berlin, 1955), Vol. 4, Part 4, p. 35]. The axes X and Y are part of a right-handed coordinate system according to the 1949 IRE standards [Proc. IRE 14, S1, 1378 (1949)].

taken into account for the first nearest Si-O neighbors, and for the first- and second-nearest O-O neighbors. In addition, angle-bending forces for the tetrahedral O-Si-O angles and for Si-O-Si angle between neighboring tetrahedra are included. There are two different Si-O distances, four different nearest-neighbor O-O distances, and four different second-neighbor O-O distances. The nearest-neighbor O-O distances correspond to the edges of the SiO_4 tetrahedra, and the second-neighbor O-O distances connect two O corners of adjacent SiO_4 tetrahedra sharing a common corner. The distances $\vec{R}(\kappa\kappa') = |\vec{R}(\kappa, 0) - \vec{R}(\kappa', L)|$ are listed in Table II, where $\vec{R}(\kappa', L)$ denotes the position vector of ion κ' , and L labels the unit cells. There are four different O-Si-O angles and only one Si-O-Si angle. The angles formed by the three ions with labels $\kappa, \kappa', \kappa''$, with the ion of type κ at the vertex of the angle are listed in Table III.

The potential energy of the crystal per unit cell is given by

$$\Phi = -M(Ze)^2/a + \Phi^{\text{S.R.}} + \Phi^{\text{A.B.}}, \quad (2.1)$$

where M is the Madelung constant, e the electronic charge, and Z an effective charge indicative of the degree of ionicity. The charge of a Si ion is taken to be $+4Ze$, and that of the O ions $-2Ze$. Denoting the various central-force short-range interaction potentials by $\phi_\alpha = \phi_\alpha(R_\alpha)$ ($\alpha = 1, 2, \dots, 10$) the

short-range contribution to the lattice energy per unit cell becomes

$$\Phi^{\text{S.R.}} = 6(\phi_1 + \phi_2) + 3(\phi_3 + 2\phi_4 + 2\phi_5 + \phi_6) + 3(\phi_7 + 2\phi_8 + \phi_9 + 2\phi_{10}). \quad (2.2)$$

From the definition of the labels α in Table II it is apparent that the first group of terms in Eq. (2.2) describes the Si-O interactions, the second group the nearest neighbor O-O interactions, and the third group the second-neighbor O-O interactions.

For the equilibrium conditions, and for the calculation of the dynamical matrix, the first and second derivatives of the interaction potentials $\phi_\alpha(R_\alpha)$ are required, which will be taken in the usual dimensionless form

$$A_\alpha = \frac{2V_c}{e^2} \left(\frac{\partial^2 \phi_\alpha(R_\alpha)}{\partial R_\alpha^2} \right)_0, \\ B_\alpha = \frac{2V_c}{e^2 R_\alpha} \left(\frac{\partial \phi_\alpha(R_\alpha)}{\partial R_\alpha} \right)_0 \quad (\alpha = 1, 2, \dots, 10). \quad (2.3)$$

$V_c = (\frac{1}{2}\sqrt{3})a^2c$ is the volume of the unit cell, and the index 0 refers to the equilibrium state.

The angle-bending contribution is represented by a sum over all angles $(\kappa\kappa'\kappa'')$ per unit cell,

$$\Phi^{\text{A.B.}} = \frac{1}{2} \sum_{\kappa\kappa'\kappa''} \phi(\kappa\kappa'\kappa''), \quad (2.4)$$

where $\phi(\kappa\kappa'\kappa'')$ denotes the three-body type deformation energy due to the change of angle between the ions $\kappa', \kappa, \kappa''$. Following a suggestion by Maradudin^{25,26} $\phi(\kappa\kappa'\kappa'')$ may be related to the change of the scalar product $\vec{R}(\kappa'\kappa) \cdot \vec{R}(\kappa''\kappa)$ as follows:

$$\phi(\kappa\kappa'\kappa'') = \frac{1}{2} G(\kappa\kappa'\kappa'') (e^2/ca^4) \\ \times [\vec{R}'(\kappa'\kappa) \cdot \vec{R}'(\kappa''\kappa) - \vec{R}(\kappa'\kappa) \cdot \vec{R}(\kappa''\kappa)]^2. \quad (2.5)$$

Here the prime denotes the position vectors in a deformed state, and the factor e^2/ca^4 has been introduced to render the angle-bending force constant $G(\kappa\kappa'\kappa'')$ dimensionless. Since in (2.5) the change of the scalar product rather than the change of the angle θ or of

$$\cos\theta = [\vec{R}(\kappa\kappa') \cdot \vec{R}(\kappa\kappa'')]/R(\kappa\kappa')R(\kappa\kappa'')$$

occurs the deformation energy $\phi(\kappa\kappa'\kappa'')$ does not represent a pure angle-bending energy, but also includes a small amount of bond stretching.

The six equilibrium conditions which express the vanishing of the external and internal stresses are obtained by minimizing the potential energy (2.1) with respect to the four structural parameters x, y, z, u and with respect to the two lattice constants a, c . This gives the relations

TABLE II. Interionic distances for short-range central-force interactions.

Type	($\kappa\kappa'$)	$R(\kappa\kappa') = \vec{R}(\kappa 0) - \vec{R}(\kappa' L) $	Label α	R_α (Å)
Si-O	(14), (19), (25), (26), (37), (38)	$[u^2 + x^2 + y^2 - xy + u(y - 2x) + r^2 z^2]^{1/2} a$	1	1.5977
	(16), (17), (28), (29), (34), (35)	$[u^2 + x^2 + y^2 - xy + 1 - 2u + (u - 1)(x + y) + r^2(z - \frac{1}{3})^2]^{1/2} a$	2	1.6159
(O-O) ₍₁₎	(49), (56), (78)	$[3y^2 + 4r^2 z^2]^{1/2} a$	3	2.6045
	(47), (58), (69)	$[3x^2 + 1 - 3x + r^2(2z - \frac{1}{3})^2]^{1/2} a$	4	2.6135
	(46), (48), (57), (59), (68), (79)	$[3x^2 + 1 - 3x + 3y^2 - 3xy + \frac{1}{9}r^2]^{1/2} a$	5	2.6364
	(45), (67), (89)	$[3(x - y)^2 + r^2(2z - \frac{2}{3})^2]^{1/2} a$	6	2.6391
(O-O) ₍₂₎	(45), (67), (89)	$[3(x - y)^2 + r^2(2z + \frac{1}{3})^2]^{1/2} a$	7	3.3348
	(49), (56), (78)	$[3y^2 + 1 - 3y + 4r^2 z^2]^{1/2} a$	8	3.4124
	(47), (58), (69)	$[3x^2 + r^2(2z - \frac{1}{3})^2]^{1/2} a$	9	3.5648
	(46), (48), (57), (59), (68), (79)	$[3(x^2 + y^2 - xy) + \frac{1}{9}r^2]^{1/2} a$	10	3.5817

$r = c/a$

$$rM_x/\sqrt{3} = (2x - y - 2u)B_1 + (2x - y + u - 1)B_2 + 3(2x - 1)B_4 + 3(2x - y - 1)B_5 + 3(x - y)(B_6 + B_7 + 3xB_9 + 3(2x - y)B_{10}), \quad (2.6a)$$

$$rM_y/\sqrt{3} = -(x - 2y - u)B_1 - (x - 2y - u + 1)B_2 + 3yB_3 - 3(x - 2y)(B_5 + B_{10}) - 3(x - y)(B_6 + B_7) + 3(2y - 1)B_8, \quad (2.6b)$$

$$M_z/2\sqrt{3}r = z(B_1 + 2B_3 + 4B_8) + (z - \frac{1}{3})B_2 + (2z - \frac{1}{3})(2B_4 + B_9) + 2(z - \frac{1}{3})B_6 + (2z + \frac{1}{3})B_7, \quad (2.6c)$$

$$M_u/\sqrt{3}r = -(2x - y - 2u)B_1 + (x + y + 2u - 2)B_2, \quad (2.6d)$$

$$M_r/2\sqrt{3} = z^2(B_1 + 2B_3 + 4B_8) + (z - \frac{1}{3})^2(B_2 + 2B_6) + (2z - \frac{1}{3})^2(B_4 + \frac{1}{2}B_9) + \frac{1}{9}(B_5 + B_{10}) + \frac{1}{2}(2z + \frac{1}{3})^2B_7, \quad (2.6e)$$

$$-r(M + rM_r)/2\sqrt{3} = [(x - \frac{1}{2}y - u)^2 + \frac{3}{4}y^2]B_1 + [(\frac{1}{2}(x + y) + u - 1)^2 + \frac{3}{4}(x - y)^2]B_2 + \frac{3}{2}y^2B_3 + (3x^2 - 3x + 1)B_4 \\ + [(\frac{3}{2}x - 1)^2 + 3(\frac{1}{2}x - y)^2]B_5 + \frac{3}{2}(x - y)^2(B_6 + B_7) + (3y^2 - 3y + 1)B_8 + \frac{3}{2}x^2B_9 + 3(x^2 + y^2 - xy)B_{10}. \quad (2.6f)$$

Here the subscripts denote the partial derivatives of the Madelung number with respect to x , y , z , u and $r = c/a$. Their numerical values are listed in Table IV. The angle-bending contributions do not

enter the equilibrium conditions because the force constants $G(\kappa\kappa'\kappa'')$ in (2.5) are essentially harmonic angle-bending force constants which represent second derivatives of the potential.

If the contributions from the second-neighbor O-O interactions are neglected ($B_7 = B_8 = B_9 = B_{10} = 0$) the equilibrium conditions (2.6) represent six

TABLE III. Angles for short-range angle-bending forces ($\cos\theta = [\vec{R}(\kappa\kappa') \cdot \vec{R}(\kappa\kappa'')]/R(\kappa\kappa')R(\kappa\kappa'')$).

Type	($\kappa\kappa'\kappa''$)	Label β	θ_β (deg)
O-Si-O	(149), (256), (378)	1	109.1901
	(146), (179), (268), (259), (348), (357)	2	110.2461
	(147), (169), (258), (269), (347), (358)	3	108.8301
	(167), (289), (345)	4	109.4908
Si-O-Si	(413), (523), (612), (713), (823), (912)	5	144.0921

TABLE IV. Madelung constant M and its derivatives with respect to the internal strain parameters u , x , y , z and with respect to the ratio $r = c/a$.

M	162.295 51
M_u	-16.004 36
M_x	164.160 69
M_y	-80.397 30
M_z	90.933 80
M_r	-48.482 04

inhomogeneous linear equations for the six unknown quantities B_1 – B_6 . Since, however, the 6×6 determinant of the corresponding homogeneous equations vanishes there is no solution of the inhomogeneous equations. Thus, in order to satisfy the equilibrium conditions it is essential to include interactions beyond the nearest-neighbor Si-O and O-O interactions.

The model described contains 26 parameters, namely the 20 first and second derivatives B_α , A_α ($\alpha = 1, 2, \dots, 10$) of the central-force short-range interactions, the five angle-bending force constants G_β ($\beta = 1, 2, \dots, 5$), and the effective charge Z . In order to reduce the number of parameters the following simplifying assumptions were made:

$$A_\alpha/R_\alpha B_\alpha = \text{const.}, \quad \alpha = 3, 4, 5, 6, \quad (2.7a)$$

$$A_\alpha = \text{const.}; \quad B_\alpha = \text{const.}, \quad \alpha = 7, 8, 9, 10, \quad (2.7b)$$

$$G_\beta = \text{const.}, \quad \beta = 1, 2, 3, 4. \quad (2.7c)$$

Assumption (2.7a) implies that the range of the short-range interactions for the four first nearest-neighbor O-O interactions is the same. If, for example, this interaction is of the Born-Mayer form, $\phi_\alpha = b_\alpha \exp(-R_\alpha/\rho_\alpha)$, (2.7a) implies that $\rho_\alpha = \text{const.}$ for $\alpha = 3, 4, 5, 6$. The assumptions (2.7b) and (2.7c) were justified by earlier trial runs, in which the parameters were determined by means of least-squares fits to experimental data as described below in Sec. III, and which showed that these relations were approximately fulfilled. This is also plausible, since (2.7b) refers to the central-force short-range interactions between the second O-O neighbors, and since (2.7c) refers to the tetrahedral bond angles. According to Tables II and III the corresponding interionic distances and bond angles do not vary greatly. Also the contributions from the second-neighbor O-O interactions to the optical frequencies and to the elastic constants are relatively small, and the least-squares fit obtained without the simplifying assumptions (2.7b) and (2.7c) is not significantly improved. Other models with additional or with fewer constraints on the parameters were also investigated and are discussed below.

Through the conditions (2.7) the number of parameters of the model is reduced to 14. The equilibrium conditions (2.6) provide six further constraints, so that the model considered has eight free parameters.

For this model the 27×27 dynamical matrix was constructed, which is defined as²⁷

$$D_{\alpha\beta}(\vec{q}, \kappa\kappa') = (m_\kappa m_{\kappa'})^{1/2} \sum_L \phi_{\alpha\beta}(L, \kappa\kappa') e^{-i\vec{q} \cdot \vec{R}(L, \kappa\kappa')}. \quad (2.8)$$

m denotes the mass of ion κ . $\phi_{\alpha\beta}(L, \kappa\kappa')$ denotes the coupling parameters, and $\vec{R}(L, \kappa\kappa')$ the difference of the position vectors between ions κ and κ' in the unit cells L and 0 , respectively. The wave vector \vec{q} ranges over the first Brillouin zone. The elastic constants were calculated from the expressions for the external strain contributions $[\alpha\beta, \gamma\lambda]$ and the internal strain contributions $(\alpha\gamma, \beta\lambda)$ ($\alpha, \beta, \gamma, \lambda = 1, 2, 3$) as given by²⁷

$$C_{\alpha\gamma\beta\lambda} = [\alpha\beta, \gamma\lambda] + [\beta\gamma, \alpha\lambda] - [\beta\lambda, \alpha\gamma] + (\alpha\gamma, \beta\lambda), \quad (2.9)$$

with

$$[\alpha\beta, \gamma\lambda] = \frac{1}{8\pi^2 V_0} \sum_{\kappa\kappa'} (m_\kappa m_{\kappa'})^{1/2} \bar{D}_{\alpha\beta, \gamma\lambda}(\kappa\kappa') \quad (2.10)$$

and

$$\begin{aligned} (\alpha\gamma, \beta\lambda) = & -\frac{1}{4\pi^2 V_0} \sum_{\kappa\kappa'} \Gamma_{\mu\nu}(\kappa\kappa') \\ & \times \sum_{\kappa''} \bar{D}_{\mu\alpha, \gamma}(\kappa, \kappa'') (m_{\kappa''})^{1/2} \\ & \times \sum_{\kappa'''} \bar{D}_{\nu\beta, \lambda}(\kappa', \kappa''') (m_{\kappa'''})^{1/2}. \end{aligned} \quad (2.11)$$

$\bar{D}_{\alpha\beta, \gamma}(\kappa\kappa')$ and $\bar{D}_{\alpha\beta, \gamma\lambda}(\kappa\kappa')$ are the first and second derivatives of the dynamical matrix (2.8) with respect to iq_γ and iq_λ , respectively, at $\vec{q} = 0$. The bar denotes that the macroscopic electric field has been removed. $\Gamma_{\mu\nu}(\kappa\kappa')$ is the inverse of $\bar{D}_{\alpha\beta}(\vec{q} = 0, \kappa\kappa')$, with the three translational degrees of freedom removed, and has the rank 24. The piezoelectric and dielectric constants are given by²⁷

$$e_{\alpha, \beta\gamma} = -\frac{e}{2\pi^2 V_0} \sum_{\kappa\kappa'\mu} \frac{Z_\kappa}{(m_\kappa)^{1/2}} \Gamma_{\alpha\mu}(\kappa\kappa') \times \sum_{\kappa''} (m_{\kappa''})^{1/2} \bar{D}_{\mu\beta, \gamma}(\kappa'\kappa''), \quad (2.12)$$

$$\epsilon_{\alpha\beta} = \delta_{\alpha\beta} + \frac{4\pi e^2}{V_0} \sum_{\kappa\kappa'} \frac{Z_\kappa Z_{\kappa'}}{(m_\kappa m_{\kappa'})^{1/2}} \Gamma_{\alpha\beta}(\kappa\kappa'). \quad (2.13)$$

Here $Z_\kappa e$ denotes the effective charge of ion κ .

The dynamical matrix and its derivatives with respect to the wave-vector components can be written as sums of the short-range central-force and angle-bending contributions and of the Coulomb contributions. The Coulomb contributions were calculated by means of Ewald's method, and the

results for the external strain parts of the elastic constants and for the quantities

$$C_{\alpha\beta\gamma}(\kappa) = -i \sum_{\kappa'} (m_{\kappa} m_{\kappa'})^{1/2} \bar{D}_{\alpha\beta\gamma}(\kappa\kappa') \quad (2.14)$$

are listed in Table V. The Coulomb contributions to the other quantities and the short-range two-body central-force and three-body angle-bending contributions are too numerous to be presented here. The Coulomb contributions to the dynamical matrix have been given before by Elcombe²¹ along the x , y , and z directions of the cartesian axes shown in Fig. 1 on the basis of slightly different structural parameters. When calculated with the input data used by Elcombe the present results agree with those of Elcombe up to the last of the five decimals given.²¹

The external and internal strain contributions to the elastic constants must satisfy the symmetry relations $[\alpha\beta, \gamma\lambda] = [\gamma\lambda, \alpha\beta]$ and $(\alpha\gamma, \beta\lambda) = (\gamma\alpha, \beta\lambda)$, which follow from the symmetry of the elastic constants for a crystal with vanishing external stresses, and from the rotational invariance conditions for the coupling parameters, respectively.²⁷ These relations are not automatically satisfied for α -quartz. If the repulsive contributions to the square brackets are eliminated by means of the equilibrium conditions (2.6e) and (2.6f), the first type of relations leads to the following relation:

$$Q_{3311} - Q_{1133} = \frac{1}{2}(M + 3\gamma M_{\gamma}). \quad (2.15)$$

The coefficients on the left-hand side are the Coulomb contributions to the external strain parts of the elastic constants as listed in Table V. The relation (2.15) also holds for the rutile structure.^{19,28}

The second type of relation follows from the

TABLE V. Coulomb contributions to the external strain parts of the elastic constants, $Q_{\alpha\beta\gamma\lambda} = (\alpha V/Z^2 e^2) \times [\alpha\beta, \gamma\lambda]^{\text{Coul}}$, and Coulomb contributions to the quantities defined in (2.14), $Q_{\alpha\beta\gamma}(\kappa) = (V/Z^2 e^2) C_{\alpha\beta\gamma}^{\text{Coul}}(\kappa)$ ($\alpha, \beta, \gamma, \lambda = 1, 2, 3$; $\kappa = 2, 4, 5$).

$\alpha\beta\gamma\lambda$	$Q_{\alpha\beta\gamma\lambda}$	$\alpha\beta\gamma(\kappa)$	$Q_{\alpha\beta\gamma}(\kappa)$
1111	-32.703 713	313 (4)	79.127 911
3333	-12.271 919	331 (4)	-84.645 764
2323	6.135 964	313 (5)	224.421 183
1212	25.419 581	331 (5)	304.419 58
1122	-83.542 863	131 (4)	-202.598 82
1133	-101.678 325	113 (4)	-285.066 65
3311	-100.530 162	121 (2)	-117.507 15
1123	4.544 185	112 (2)	-89.852 126

rotational-invariance conditions for the coupling parameters, which can for a stress-free crystal be written²⁷

$$C_{\alpha\beta\gamma}(\kappa) = C_{\alpha\gamma\beta}(\kappa) \quad (\alpha, \beta, \gamma = 1, 2, 3), \quad (2.16)$$

where

$$C_{\alpha\beta\gamma}(\kappa) = \sum_{\kappa'} \phi_{\alpha\beta\gamma} X_{\gamma}(\kappa\kappa'). \quad (2.17)$$

Here $X_{\gamma}(L, \kappa\kappa')$ denotes the γ component of $\vec{R}(L, \kappa\kappa') = \vec{R}(L\kappa) - \vec{R}(0\kappa')$. If the short-range contributions to (2.16) are eliminated by means of the equilibrium conditions (2.6a)–(2.6d), the conditions (2.16) lead to the four relations

$$Q_{313}(4) - Q_{331}(4) = (\pi/2\sqrt{3}) \gamma M_x, \quad (2.18a)$$

$$Q_{313}(5) - Q_{331}(5) = (\pi/2\sqrt{3}) \gamma M_y, \quad (2.18b)$$

$$Q_{131}(4) - Q_{113}(4) = (\pi/2\sqrt{3}) M_z, \quad (2.18c)$$

$$Q_{121}(2) - Q_{112}(2) = (\pi/2) \gamma M_u. \quad (2.18d)$$

The coefficients on the left-hand side are the Coulomb contributions to the quantities (2.17) and are also listed in Table V. All other rotational invariance conditions are either automatically satisfied or are equivalent to the equilibrium conditions and to (2.18a)–(2.18d).

Approximate derivatives of the Madelung number were calculated by means of numerical differentiation of the values obtained from Ewald's method, and were found to agree to within a few percent with the values obtained from (2.15) and (2.18a)–(2.18d), with the $Q_{\alpha\beta\gamma}$ obtained directly by Ewald's method. Since the $Q_{\alpha\beta\gamma}$ involve analytical differentiation they are more accurate than the derivatives of the Madelung number obtained by numerical differentiation. Therefore the derivatives of M as calculated from the $Q_{\alpha\beta\gamma}$ by means of (2.15) and (2.18a)–(2.18d) are given in Table IV and were used in all calculations.

III. DETERMINATION OF PARAMETERS

The eight free parameters of the model were determined from a least-squares fit of the calculated six elastic constants and the squares of the frequencies of the four Raman-active $A(\Gamma_1)$ modes, of the four transverse ir-active $B_T(\Gamma_{2T})$ modes, and of the eight transverse Raman- and ir-active $E_T(\Gamma_{3T})$ modes to the 22 experimental data^{29–31} at 300 °K.

In order to convert all experimental data into dimensionless quantities with equal relative weight the expression

$$\sum_{i=1}^n (X_i^{\text{exp}} - X_i^{\text{calc}})^2 / (X_i^{\text{exp}})^2,$$

with weight factors $(X_i^{\text{exp}})^{-2}$, was minimized with

respect to the eight free parameters. The results for all 26 parameters of the model are listed in Table VI.

Since both $A_\alpha > 0$ and $B_\alpha > 0$ for $\alpha = 1, 2$ and $\alpha = 7, \dots, 10$ the short-range interactions for the Si-O neighbors and for the second-nearest O-O neighbors do not correspond to a repulsive potential. The dimensionless second derivatives A_α for the nearest-neighbor O-O interactions are approximately equal and about 20 times smaller than the Si-O interactions, and about eight times larger than the second-neighbor O-O interactions.

For the Si-O interactions the parameters are approximately 30% smaller, and for the nearest-neighbor O-O interactions they are approximately 60% larger than the parameters in the rigid-ion model of Elcombe.²² The effective charge of Elcombe's model is twice the value of Table VI. These differences are most likely due to the simplifying assumptions underlying Elcombe's model²² and to the different fitting procedures used. Elcombe uses weight factors inversely proportional to the square of the errors of the optical frequencies and includes the LO frequencies, but not the elastic constants in the least-squares fit. In the present work the LO frequencies were excluded from the least-squares fit since they depend more strongly on the electronic polarizabilities, which are neglected in the present model, than the TO frequencies.

IV. JUSTIFICATION OF MODEL

In order to justify the model adopted least-squares fits to the 16 optical frequencies (A, B_T, E_T) and to the six elastic constants were

TABLE VI. Short-range parameters A_α, B_α ($\alpha = 1, 2, \dots, 10$), angle-bending force constants G_β ($\beta = 1, 2, \dots, 5$), and effective charge Z for modified rigid-ion model C6A2, based on the assumptions (2.7a)–(2.7c), and determined from least-squares fit to 16 TO frequencies and six elastic constants.

α	A_α ^a	B_α ^b	β	G_β ^c	Z
1	516.1	32.8	1	39.3	0.236
2	461.6	34.0	5	66.4	
3	23.8	-11.1			
4	25.9	-12.1			
5	26.0	-12.0			
6	25.2	-11.7			
7	0.291	0.075			

^a $A_7 = A_8 = A_9 = A_{10}$.

^b $B_7 = B_8 = B_9 = B_{10}$.

^c $G_1 = G_2 = G_3 = G_4$.

made for three additional models with fewer or more parameters. In Table VII the individual contributions to the residual sum of squares arising from the TO frequencies [$S^2(\text{TO})$] and from the elastic constants [$S^2(\text{elast})$] and the total residual sum of squares, and the standard deviation $\sigma = S(\text{tot}) / (n - p)^{1/2}$ for the $n - p$ degrees of freedom are listed for the four models considered. Here p denotes the number of free parameters of the models. Also included in Table VII are the residual sum of squares for the 12 LO modes (B_L, E_L), which were not included in the least-squares fit.

The models considered are all modified rigid-ion models of the type described in Sec. II, and are different in that other assumptions instead of (2.7a) and (2.7c) are made. The four models are (I) a six-parameter central-force model without angle-bending forces, denoted by C6, obtained by setting all angle-bending force constants in the above model equal to zero; (II) a nine-parameter central-force model without angle-bending forces, denoted by C9, without the three constraints (2.7a), so that the eight parameters A_α, B_β ($\alpha = 3, 4, 5, 6$) for the nearest-neighbor O-O interactions are independently varied; (III) the eight-parameter model characterized by the constraints (2.7a)–(2.7c), denoted by C6A2, representing the final selection for the present paper; and (IV) an 11-parameter model with five independent angle-bending forces, denoted by C6A5, and obtained by deleting the constraints (2.7c).

The fact that the smallest value of the σ occurs for model C6A2 suggests that this model is the best one among the four models considered. In order to test whether it is also necessary to use this model, that is whether the standard deviation is sufficiently smaller than for the other models, the F test³³ was applied to the comparison of models II, III, and IV with model I. The quantity

$$\{ [S_{\text{tot}}^2(\text{I}) - S_{\text{tot}}^2(K)] / (p_K - p_I) \} / [S_{\text{tot}}^2(\text{I}) / (n - p_K)],$$

where p_K denotes the number of free parameters of model K , has the values 1.73, 3.50, and 1.79, for models II, III, and IV respectively. From the F tables³⁴ one obtains for a probability level of 95% for the corresponding F values: 3.41, 3.74, and 3.20, respectively. Therefore models II and IV are not statistically significant at the 95% level, whereas the two additional parameters of model III improve the least-squares fit at a probability level close to 95%. This justifies the selection of this model for the subsequent calculations.

As the data in Table VII indicate for all four models the residual sum of squares for the 12 LO modes is smaller than for the 16 TO modes, al-

TABLE VII. Residual sum of squares

$$S^2 \sum_{i=1}^n (X_i^{\text{exp}} - X_i^{\text{calc}})^2 / (X_i^{\text{exp}})^2$$

for TO and LO frequencies and for elastic constants, and standard deviation $\sigma = S(\text{tot}) / (n - p)^{1/2}$ for the following: (A) Four versions of the modified rigid-ion model, with parameters determined from 16 TO frequencies and six elastic constants ($n = 22$). (B) The final version C6A2 of the present modified rigid-ion model, with parameters determined from 16 TO and 12 LO frequencies ($n = 28$). (C) The final version C6A2 of the present modified rigid-ion model, with parameters determined from 16 TO and 12 LO frequencies and six elastic constants ($n = 34$). (D) Elcombe's modified rigid-ion model (Ref. 22), with parameters determined from 16 LO and 12 TO frequencies ($n = 28$). The following abbreviations are used for the models: C6, six-parameter central-force model; C9, nine-parameter central force model; C6A2, model C6 with two additional angle-bending force constants; C6A5, model C6 with five additional angle-bending force constants.

Model	A		B		C	D	
	C6 ($p = 6$)	C9 ($p = 9$)	C6A2 ($p = 8$)	C6A5 ($p = 11$)	C6A2 ($p = 8$)	Elcombe (Ref. 22) ($p = 5$)	
$S^2(\text{TO})$	0.268	0.292	0.154	0.203	0.102	0.179	0.223
$S^2(\text{LO})$	(0.163) ^a	(0.149) ^a	(0.103) ^a	(0.126) ^a	0.038	0.060	0.209
$S^2(\text{elast})$	0.482	0.244	0.345	0.211	(4.447) ^a	0.337	(1.801) ^{a,b}
$S^2(\text{tot})$	0.750	0.536	0.499	0.414	0.140	0.576	0.432
σ	0.217	0.203	0.189	0.194	0.084	0.149	0.137

^a Not included in least-squares fit, in $S^2(\text{tot})$ and in σ .

^b Calculated without c_{13} and by choosing the correct sign for the calculated value of c_{14} .

though they were not included in the least-squares fit. This may be attributed predominantly to the fact that the TO-LO mode splitting is small in α -quartz and is indicative of the smallness of electronic polarizability effects.

The data in Table VII indicate further that the reduction of $S^2(\text{elast})$ from the value of 0.482 for model I-C6 resulting from the introduction of additional parameters is smallest for the selected model III-C6A2. The other two models (II and IV) lead to smaller values for $S^2(\text{elast})$, but to larger values of $S^2(\text{TO})$ and $S^2(\text{LO})$. Especially model IV which contains five different angle-bending forces gives a much better fit for the elastic constants than model III, whereas the fit for the optical frequencies deteriorates somewhat. In spite of this obvious advantage of model IV for fitting the elastic constants, model III will be used subsequently because it is the statistically most plausible model for providing a good over-all fit.

In order to compare the present model with the modified rigid-ion model of Elcombe²² in Table VII the residual sums of squares and the standard deviations are also included for the final version C6A2, but with their parameters determined (as in Elcombe's work) from the 16 TO and 12 LO frequencies (column B) and with their parameters determined from all 34 TO and LO frequencies and elastic constants (column C). As expected, in both cases $S^2(\text{TO})$ and $S^2(\text{LO})$ are significantly

smaller than for Elcombe's model, and in the second case the total standard deviation σ is only insignificantly larger than for Elcombe's model without the contribution from the elastic constants. The large values of $S^2(\text{elast})$ for those cases, for which the elastic constants were not included in the least-squares fit indicate that it is not possible to account for the elastic constants of α -quartz, if the parameters of the model are determined from optical data only. Surprisingly, Elcombe's Born-von Kármán model gives values for $S^2(\text{TO})$ and $S^2(\text{LO})$ about three to four times smaller than her rigid-ion model, but $S^2(\text{elast})$ is significantly larger in that case.

If the eight parameters of model C6A2 are determined from a least-squares fit to the six elastic constants only, $S^2(\text{elast})$ is reduced by about one order of magnitude, but $S^2(\text{TO})$ and $S^2(\text{LO})$ are increased by about one order of magnitude. Thus it is possible to obtain a very good fit for the elastic constants, however, at the expense of a poor fit for the optical frequencies with calculated frequencies being up to three times too large.

As has been shown by Miller and Axe³⁵ the elastic constants and the Raman frequencies are related via the internal strain contributions as given below in Eq. (4.1). Therefore the procedure of fitting the parameters of the model either to the optical frequencies or to the elastic constants only must be considered as inconsistent.

TABLE VIII. Optical-mode frequencies^a (cm⁻¹) at zero wave vector, and elastic constants^b (10¹² dyn/cm²).

Representation	Experimental ^a	Theoretical
ω_A (Raman)	207	203.9
	356	375.0
	466	474.6
	1082	1127.3
ω_{B_T} (ir)	364	379.8
	495	531.4
	778	745.7
ω_{E_T} (Raman and ir)	1080	1134.7
	128	136.3
	265	256.2
	394	378.0
	450	494.6
	697	667.9
	795	775.0
	1072	1086.9
	1162	1135.2
	ω_{B_L} ^c (ir)	388
547		545.5
790		754.8
ω_{E_L} ^c (Raman and ir)	1240	1153.4
	129	136.4
	270	256.9
	403	380.6
	510	511.5
	699	668.5
	809	784.0
	1161	1086.9
	1236	1154.2
	c_{11}	0.8680
c_{33}	1.0575	0.655
c_{44}	0.5820	0.492
c_{66}	0.3988	0.338
c_{12}	0.0704	0.0796
c_{13}	0.119	0.103
c_{14}	-0.180	-0.117

^a Experimental optical data are from Spitzer and Kleinman (Ref. 31), except for the two lowest E modes. Their transverse frequencies are from Krishnan (Ref. 29) and D. Krishnamurty (Ref. 30); their longitudinal frequencies have been calculated from the transverse frequencies and from the frequency dependence of the dielectric constant by M. M. Elcombe (Ref. 22).

^b Experimental elastic data are from Ref. 32.

^c Not included in the least-squares fit.

V. NUMERICAL RESULTS AND DISCUSSION

In Tables VIII and IX the optical mode frequencies, the elastic constants, and the dielectric and piezoelectric constants as calculated from the selected eight-parameter model C6A2 are compared with the experimental data. For the optical frequencies discrepancies up to 10%, and for the elastic constants discrepancies up to 35% (for c_{33} and c_{14}) occur, but on the whole the agreement for both sets of data is satisfactory. The calculated

TABLE IX. Calculated and experimental dielectric and piezoelectric constants (C/m^2) of α -quartz.

	Calc	Exp ^a
ϵ_x	3.82	4.44 ^b
ϵ_z	3.94	4.64 ^b
e_{11}	0.050	0.171
e_{14}	-0.016	-0.0406

^a R. Bechmann, Phys. Rev. **110**, 1060 (1958).

^b Adiabatic values.

dielectric constants ϵ_x and ϵ_z (not included in the least-squares fit) are 14% and 15% smaller than the experimental values, respectively. Because of the neglect of electronic polarizability in the present model this discrepancy is, of course, not surprising. The piezoelectric constants (which were also not included in the least-squares fit) show the largest discrepancies, but for both e_{11} and e_{14} the correct sign is predicted. As for the dielectric constants the discrepancy is most likely to arise from neglecting the electronic polarizability.

As mentioned above, very good agreement of the elastic constants (within a few percent) is obtained if the parameters of the model are determined from a least-squares fit to the elastic constants only. The agreement for the piezoelectric constants (not included in the least-squares fit) is also considerably improved, with discrepancies of 10% for e_{11} and 35% for e_{14} . However, because of the drastic deterioration mentioned above resulting for the optical frequencies this fitting procedure is not feasible.

According to Miller and Axe³⁵ the internal strain contributions to the elastic constants as defined in Eq. (2.11) can be written in tensor notation ($\alpha, \gamma, \mu, \delta = 1, 2, 3$)

$$(\alpha\gamma, \mu\delta) = - \sum_j F_{\alpha\gamma}(j) F_{\mu\delta}(j) / \omega^2(j), \quad (5.1)$$

where the sum is to be extended over the Raman-active modes at the zone center. The coefficients $F_{\alpha\gamma}(j)$ are sums over products of the first derivatives of the elements of the dynamical matrix with respect to wave vector, with the components $e_{\beta\kappa}(j)$ of the eigenvectors of the dynamical matrix.³⁵ From group-theoretical arguments it can be shown that the internal strain contributions to c_{33} and c_{13} , and to c_{44} , c_{66} , and c_{14} depend only on the modes belonging to the A representation, and to the E representation, respectively. The remaining constants c_{11} and c_{12} depend on internal strain contributions arising from modes of both A and E representations.

In view of an earlier suggestion by Miller and Axe³⁵ (which has been revoked later³⁶) that the elastic anomaly in β -quartz near the α - β phase transition arises predominantly from a single contribution of a soft mode in Eq. (4.1), it was of interest to calculate the individual mode contributions in the sum in Eq. (4.1). The results of these calculations are shown in Table X and indicate that in all cases almost all modes contribute significantly to the internal strain parts of the elastic constants. Exceptions are the softest mode of the A representation ($\nu=207\text{ cm}^{-1}$) and the three intermediate modes of the E representation with frequencies of 265, 450, and 795 cm^{-1} . None of these frequencies contributes significantly to any of the internal strain parts, except the mode with frequency 795 cm^{-1} , which gives the largest contribution to the internal strain part of c_{44} .

The diagonal elements of the static dielectric constant tensor are for the rigid-ion model given by²⁷

$$\epsilon_{\alpha} = 1 + 4\pi \sum_j \frac{P_{\alpha}^2(j)}{\omega^2(j)} \quad (\alpha = x, y, z), \quad (5.2)$$

where $P_{\alpha}(j)$ denotes the components of the dipole moment of the j th normal mode at the zone center, and the sum is over the ir-active modes. In α -quartz ϵ_x depends only on the $E_T(\Gamma_{3T})$ modes, and ϵ_z only on the $B_T(\Gamma_{2T})$ modes. It was found that all four B_T modes contribute significantly to ϵ_z . For the E_T modes five modes contribute substantially to ϵ_x , but the three modes with calculated

frequencies of 128, 697, and 1072 cm^{-1} possess small dipole moments and give negligible contributions (smaller than 1%) to ϵ_x .

Also listed in Table X are the total internal strain contributions. They are of comparable magnitude and opposite sign as the external strain contributions, so that the resulting total elastic constants in Table VIII are numerically much smaller than either the external or the internal contributions. This fact may explain in part the relatively large discrepancies between calculated and observed elastic constant values. In addition, the neglect of electronic polarizability may have more serious consequences for the elastic (and piezoelectric) constants than for the optical mode frequencies, since the internal strain contributions may be significantly affected by electronic polarizabilities.³⁷

In Table XI the calculated Cauchy differences $c_{12} - c_{66}$ and $c_{13} - c_{44}$ are compared with the experimental values. Fair agreement, with discrepancies of approximately 20%, is found. Since for central forces the Cauchy relations hold for the external strain contributions to the elastic constants,²⁷ the data in Table XI indicate further that for $c_{12} - c_{66}$ half of the calculated Cauchy difference, and that for $c_{13} - c_{44}$ about one-third of the Cauchy difference arises from the angle-bending forces.

In Fig. 2 the calculated phonon dispersion curves of the acoustic branches and of the four lowest optical branches with wave vector parallel to the c axis are compared with the experimental data

TABLE X. Contributions $\Delta c_{\mu\nu}(j)$ ($\mu, \nu=1, 2, \dots, 6$; Voigt notation) from individual normal modes at the Brillouin-zone center to the internal strain contributions of the elastic constants according to Eq. (4.1) [$\Delta C_{\alpha\gamma, \mu\delta}(j) = F_{\alpha\gamma}(j)F_{\mu\delta}(j)/\omega^2(j)$, $\alpha, \gamma, \mu, \delta=1, 2, 3$; tensor notation], and total internal strain contributions to the elastic constants (in 10^{12} dyn/cm^2).

Representation	$\omega(j)$ (cm^{-1}) (calc)	Δc_{11}	Δc_{33}	Δc_{44}	Δc_{66}	Δc_{12}	Δc_{13}	Δc_{14}
A	204	-0.0086	-0.0494	0	0	-0.0086	0.0206	0
	375	-0.6873	-0.6380	0	0	-0.6873	-0.6622	0
	475	-0.7920	-0.9922	0	0	-0.7920	-0.8865	0
	1127	-0.1285	-0.2764	0	0	-0.1285	0.1885	0
E^a	136	-0.1411	0	-0.2640	-0.1411	0.1411	0	-0.1930
	256	-0.0006	0	-0.0562	-0.0006	0.0006	0	0.0057
	378	-0.1099	0	-0.0519	-0.1099	0.1099	0	-0.0755
	495	-0.0002	0	-0.0001	-0.0002	0.0002	0	-0.0001
	668	-0.1472	0	-0.0029	-0.1472	0.1472	0	-0.0206
	775	-0.0040	0	-0.6000	-0.0040	0.0040	0	-0.0491
	1087	-0.1887	0	-0.0087	-0.1887	0.1887	0	-0.0405
	1135	-0.1522	0	-0.0927	-0.1552	0.1522	0	0.1188
Total		-2.3603	-1.9560	-1.0765	-0.7439	-0.8725	-1.3396	-0.2543

^a In calculating the internal strain contributions to the elastic constants the macroscopic field in the E_L modes has to be omitted, so that the contributions from E_T and E_L modes are the same.

TABLE XI. Calculated external and internal strain contributions and calculated and experimental Cauchy differences (in 10^{12} dyn/cm²).

	Theoretical			Experimental
	Δc^{ext}	Δc^{int}	Δc^{tot}	Δc
$c_{12} - c_{66}$	-0.129	-0.129	-0.258	-0.328
$c_{13} - c_{44}$	-0.126	-0.264	-0.390	-0.463

of Elcombe.²² For the optical branches very good agreement is found. The three acoustic branches exhibit the correct shape and position of the maximum of the highest branch, but lie up to 20% too low. Apparently, this results from the fact that the calculated elastic constants c_{33} and c_{44} are about 38 and 15% too small, respectively. The over-all agreement of the calculated curves in Fig. 2 with the experimental data is considerably better than for either of the two theoretical models investigated by Elcombe.²²

The phonon dispersion curves of all branches shown in Fig. 3 for wave vectors parallel to the x , y , and z axes of the Cartesian coordinate system of Fig. 1 agree qualitatively with those calculated by Elcombe,²² but there are several significant quantitative differences. The most conspicuous feature is the large frequency gap between about 24×10^{12} and 32×10^{12} sec⁻¹, which has also been noted by Elcombe.²²

The phonon density of states has been calculated by the root sampling method from a total of 1000 wave-vector points in the entire Brillouin zone by using a mesh width of $\Delta\nu = 0.25 \times 10^{12}$ sec⁻¹. The most noteworthy features of the resulting histogram in Fig. 4 are the relatively broad band between 2×10^{12} and 24×10^{12} sec⁻¹, with various pronounced peaks in this region, and the unusually large peak near 34×10^{12} sec⁻¹. It appears that there are two additional small gaps at the high-frequency end of the spectrum, but it could not be decided whether they arise from the limited resolution of the calculation.

The specific heat was calculated as a function of temperature from the same set of wave-vector points in the Brillouin zone as the frequency spectrum. The Debye temperature calculated from these data with the aid of the tables of Beattie³⁸ is compared in Fig. 5 with the experimental curve, calculated from the specific heat for constant volume.³⁹⁻⁴¹ The most noteworthy feature is the unusually large increase in Θ by a factor of about 2, which may be attributed to the large spread of the frequency spectrum and which is well accounted for by the calculated curve. While the agreement

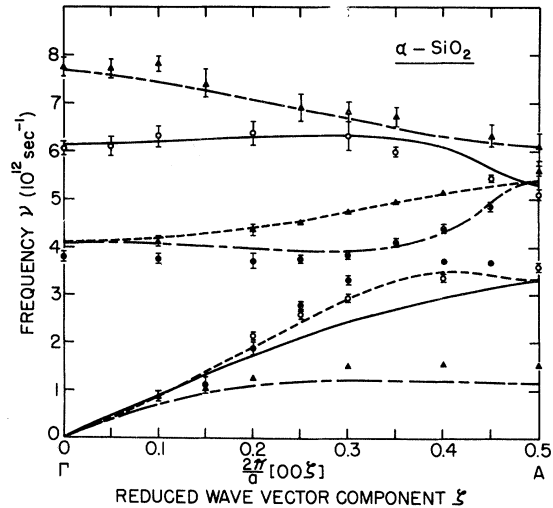


FIG. 2. Comparison of calculated phonon dispersion curves with wave vector parallel to c axis for α -SiO₂ with experimental data of Elcombe (Ref. 22). Solid lines and open circles belong to the irreducible representation Δ_1 corresponding to longitudinal vibrations; dashed lines and full circles belong to the irreducible representation Δ_2 corresponding to transverse vibrations; long-short dash lines and full triangles belong to the irreducible representation Δ_3 corresponding to transverse vibrations.

between 100 and 500 °K (from 2×10^{12} – 10×10^{12} sec⁻¹) is excellent, below 100 °K the calculated curve is up to 10% smaller than the experimental curve. This is to be expected since, with the exception of c_{12} , the calculated elastic constants are smaller than the experimental values. Therefore the acoustic branches in directions other than [001] may also be expected to be smaller than the actual values, although the difference should be considerably smaller than for the acoustic branches in [001]. However, the location of the minimum of the Debye temperature curve is well accounted for by the theoretical curve. The good agreement found in the range 100–500 °C may be taken as an indication of the correctness of the calculated dispersion curves for the optical branches. The discrepancy above 500 °K arises probably from anharmonic effects and from the occurrence of the α - β phase transformation at 850 °K.

VI. SUMMARY AND CONCLUSIONS

The model presented here for α -quartz gives considerably improved over-all agreement for the optical and elastic properties as well as for the phonon dispersion curves as compared with previous investigations. However, in spite of the

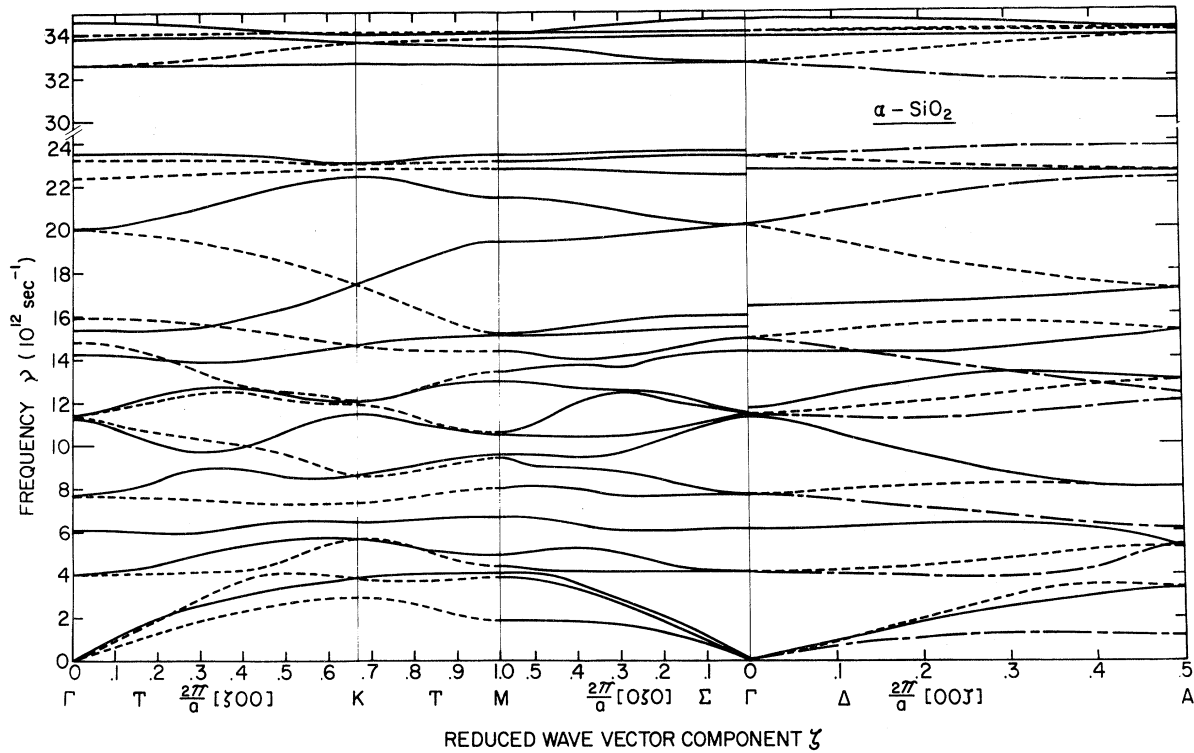


FIG. 3. Calculated phonon dispersion curves of α - SiO_2 along principal symmetry directions. The reduced wave vector coordinate ζ is referred to Cartesian axes. In [100], solid lines correspond to the irreducible representation T_1 and the dashed lines to the irreducible representation T_2 ; in [001], solid lines correspond to Δ_1 , dashed lines to Δ_2 , long-short dash lines to Δ_3 .

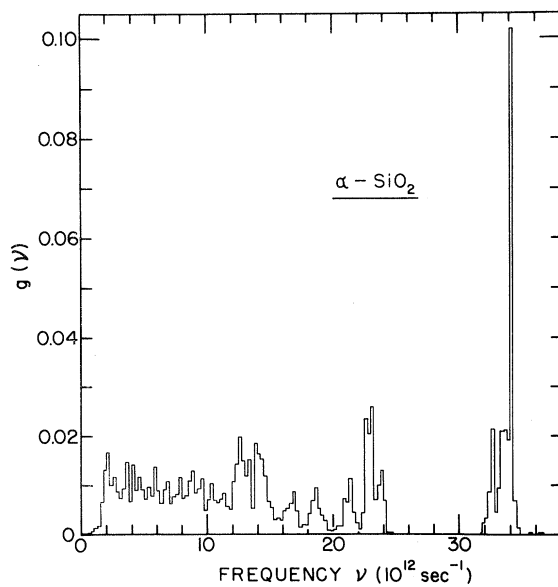


FIG. 4. Phonon density of states for α - SiO_2 . Histogram was obtained from 1000 wave-vector points in the Brillouin zone by using a mesh width for the frequency of $\Delta\nu = 0.25 \times 10^{12} \text{ sec}^{-1}$ and is normalized according to $\int g d\nu = 1$.

more elaborate nature of the present model the agreement for the optical frequencies alone is only moderately improved as compared with Elcombe's model.²² It is not possible to attribute the im-

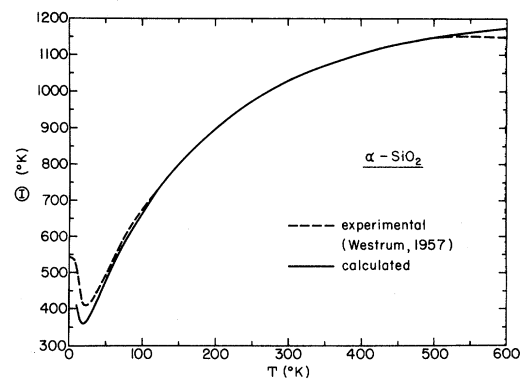


FIG. 5. Comparison of calculated Debye temperature of α - SiO_2 with experimental results obtained from specific heat data of E. F. Westrum (private communication), quoted by R. C. Lord and J. C. Morrow, *J. Chem. Phys.* **26**, 230 (1957), and of N. S. Natarajan, *Indian J. Pure Appl. Phys.* **5**, 372 (1967).

provement to any particular feature of the model. One crucial factor, however, is the determination of the parameters of the model from a least-squares fit to both optical and elastic data, but the differentiated nature of the short-range repulsive interactions and the consistency of the model achieved by considering the equilibrium and rotational-invariance conditions are also necessary features. Neglecting the equilibrium and rotational-invariance conditions leads to inconsistencies, resulting, for example, in contributions to the internal strain parts of the elastic constants from all optical modes, including the *A* and *B* representations, whereas according to the group-theoretical considerations of Miller and Axe²⁸ only the modes of the *E* representation can contribute. The importance of other features, such as the relation between the second-neighbor O-O interactions and the equilibrium conditions, or the interrelation between optical frequencies and elastic constants via their internal strain contributions, requiring simultaneous consideration of both, have been pointed out above.

The intermediate character of the chemical bond in quartz, considered partly ionic and partly covalent, is well known.⁷ The small effective ionic charge of 0.94 electrons for the Si ions apparently confirms the weakly ionic nature of α -SiO₂. Although thereby the Coulomb contributions are gen-

erally rendered small, they are still essential for a good fit to all data, so that a pure short-range force model is inadequate.

The limitations of the present model are, of course, the neglect of electronic polarizability and of thermal and anharmonic effects. The success of the short-range force model of Kleinman and Spitzer⁷ with two effective charges in accounting for the intensities of the Raman- and ir-active *A* and *B* modes, respectively, seems to suggest that a conventional shell model with polarizable O ions would not be sufficient, but that the effect of the exchange charge accumulated along each of the Si-O bonds must be included. On the other hand, the explanation of the elastic anomaly and the mode softening mechanism in relation to the α - β phase transformation require explicit inclusion of anharmonic effects.^{36,42} The extension of the present model to incorporate both kinds of effects remains as a task for the future.

ACKNOWLEDGMENTS

The authors would like to thank Dr. E. F. Westrum for communicating to them the results of his specific-heat measurements prior to publication. The use of the Computer Facilities of The Pennsylvania State University is also gratefully acknowledged.

*Work supported by the Air Force Cambridge Laboratories under Contract No. F19628-73-C-108.

¹B. D. Saksena, Proc. Indian Acad. Sci. A 12, 93 (1940).

²B. D. Saksena, Proc. Indian Acad. Sci. A 16, 270 (1942).

³B. D. Saksena, Proc. Indian Acad. Sci. A 22, 379 (1945).

⁴B. D. Saksena and H. Narain, Proc. Indian Acad. Sci. A 30, 128 (1949).

⁵B. D. Saksena and S. S. Bhatnagar, Proc. Indian Acad. Sci. A 30, 308 (1949).

⁶J. Barriol, J. Phys. (Paris) 7, 209 (1946).

⁷D. A. Kleinman and W. G. Spitzer, Phys. Rev. 125, 16 (1962).

⁸J. Etchepare, M. Merian, and L. Smetankine, J. Chem. Phys. 60, 1873 (1974).

⁹J. F. Scott and S. P. S. Porto, Phys. Rev. 161, 903 (1967).

¹⁰J. D. Masso, C. Y. She, and D. F. Edwards, Phys. Rev. B 1, 4179 (1970).

¹¹B. D. Saksena, Proc. Indian Acad. Sci. A 19, 357 (1944).

¹²D. J. Weidner and G. Simmons, J. Geophys. Res. 77, 826 (1972).

¹³B. D. Saksena and K. G. Srivastava, Indian J. Phys. 22, 475 (1948).

¹⁴B. D. Saksena and K. G. Srivastava, Proc. Indian Acad. Sci. 28, 423 (1948).

¹⁵S. Machlup and M. E. Christopher, J. Appl. Phys. 32, 1387 (1961).

¹⁶C. L. Julian and F. O. Lane, Jr., J. Appl. Phys. 39, 2316 (1968).

¹⁷S. Karasawa, Jpn. J. Appl. Phys. 13, 799 (1974).

¹⁸M. E. Striefler and G. R. Barsch, J. Phys. Chem. Solids 33, 2229 (1972).

¹⁹M. E. Striefler and G. R. Barsch, Phys. Status Solidi B 59, 205 (1973).

²⁰M. E. Striefler and G. R. Barsch, Phys. Status Solidi B 67, 143 (1975).

²¹M. M. Elcombe, Ph.D. thesis (Cambridge University, 1966) (unpublished).

²²M. M. Elcombe, Proc. Phys. Soc. Lond. 91, 947 (1967).

²³R. W. G. Wyckoff, *Crystal Structures* (Interscience, New York, 1963), Vol. 1, p. 312.

²⁴G. S. Smith and L. E. Alexander, Acta Crystallogr. 16, 462 (1963).

²⁵A. A. Maradudin (unpublished).

²⁶S. S. Jaswal and J. R. Hardy, Phys. Rev. 171, 1090 (1968).

²⁷M. Born and K. Huang, *Dynamical Theory of Crystal Lattices* (Clarendon, Oxford, 1954).

²⁸G. C. Cran and M. J. L. Sangster, J. Phys. C 5, 1008 (1972).

²⁹R. S. Krishnan, Nature (Lond.) 155, 452 (1945).

³⁰D. Krishnamurti, Proc. Indian Acad. Sci. A 47, 276 (1958).

³¹W. G. Spitzer and D. A. Kleinman, Phys. Rev. 121, 1324 (1961).

- ³²H. J. McSkimin, P. Andreatch, Jr., and R. N. Thurston, *J. Appl. Phys.* 36, 1624 (1965).
- ³³N. R. Draper and H. Smith, *Applied Regression Analysis* (Wiley, New York, 1966), p. 24.
- ³⁴Reference 33, p. 306.
- ³⁵P. B. Miller and J. D. Axe, *Phys. Rev.* 163, 924 (1967).
- ³⁶J. D. Axe and G. Shirane, *Phys. Rev. B* 1, 342 (1970).
- ³⁷J. D. Axe, *Phys. Rev.* 139, A1215 (1965).
- ³⁸J. A. Beattie, *J. Math. Phys.* 6, 1 (1926).
- ³⁹E. F. Westrum (private communication); quoted in Ref. 40.
- ⁴⁰R. C. Lord and J. C. Morrow, *J. Chem. Phys.* 26, 230 (1957).
- ⁴¹N. S. Natarayan, *Indian J. Pure Appl. Phys.* 5, 372 (1967).
- ⁴²J. F. Scott, *Phys. Rev. Lett.* 21, 907 (1968).